Received 16 October 1998; accepted 8 February 1999.

1. Hobbs, P. V. *Ice Physics* (Clarendon, Oxford, 1974).
2. Gaffney, E. S. Water ice polymorphs and their significance on planetary surfaces. *Icarus* **44,** 511–519 (1980).
3. Hemley, R. J., Chen, L. C. & Mao, H. K. New transformations between crystalline and amorphous ice. *Nature* **338,** 638–640 (1989).
4. Finney, J. L., Lobban, C., Klotz, S. & Besson, J. M. in *Collected Abstracts of the XVII Congress and General Assembly* (ed. Griffin, J. F.) C-534 (IUCr, Seattle, 1996).
5. Finney, J. L., Lobban, C., Klotz, S., Besson, J. M. & Hamel, G. in *ISIS 96—Rutherford Appleton Laboratory Report RAL 96-050* (ed. Taylor, A. D.) Vol. A17 (Chilton, UK, 1996).
6. Kuhs, W. F., Finney, J. L., Veltier, C. & Bliss, D. V. Structure and hydrogen ordering of ices VI, VII, and VIII by neutron powder diffraction. *J. Chem. Phys.* **81,** 3612–3623 (1984).
7. Nelmes, R. J. *et al.* Neutron diffraction study of the structure of deuterated ice VIII to 10 GPa. *Phys. Rev. Lett.* **71,** 1192–1195 (1993).
8. Besson, J. M. *et al.* Variation of interatomic distances in ice VIII to 10 GPa. *Phys. Rev. B* **49,** 12540–12550 (1994).
9. Nelmes, R. J. *et al.* Multi-site disordered structure of ice VII to 20 GPa. *Phys. Rev. Lett.* **81,** 2719–2722 (1998).
10. Besson, J. M. *et al.* Structural instability in ice VIII under pressure. *Phys. Rev. Lett.* **78,** 3141–3144 (1997).
11. Balagurov, A. M. *et al.* Neutron-diffraction study of phase transitions of high-pressure metastable ice VIII. *JETP Lett.* **53,** 30–34 (1991).
12. Mishima, O., Calvert, L. D. & Whalley, E. *Nature* **314,** 76–78 (1985).
13. Bellissent-Funel, M.-C., Teixera, J. & Bosio, L. Structure of high-density amorphous water. II. Neutron scattering study. *J. Chem. Phys.* **87,** 2231–2235 (1987).
14. Bizid, A., Bosio, O., Defrain, A. & Oumezzine, M. Structure of high-density amorphous water. I. X-ray diffraction study. *J. Chem. Phys.* **87,** 2225–2230 (1987).
15. Bosio, L., Johari, G. P. & Teixera, J. X-ray study of high-density amorphous water. *Phys. Rev. Lett.* **56,** 460–463 (1986).

Acknowledgements. This work was supported by the UK EPSRC and the UK CCLRC, as well as the French Institut National des Sciences de l'Univers and the French Commissariat à l'Energie Atomique.

Correspondence and requests for materials should be addressed to S.K. (e-mail: stk@pmc.jussieu.fr).

Low-temperature superplasticity in nanostructured nickel and metal alloys

S. X. McFadden*, R. S. Mishra*, R. Z. Valiev†, A. P. Zhilyaev† & A. K. Mukherjee*

** Department of Chemical Engineering and Materials Science, University of California, Davis, California 95616, USA*
† Institute of Physics and Advanced Materials, Ufa State Aviation Technical University, 12, K. Marx Street, Ufa, 450000 Russia

Superplasticity—the ability of a material to sustain large plastic deformation—has been demonstrated in a number of metallic, intermetallic and ceramic systems. Conditions considered necessary for superplasticity[1] are a stable fine-grained microstructure and a temperature higher than 0.5 T_m (where T_m is the melting point of the matrix). Superplastic behaviour is of industrial interest, as it forms the basis of a fabrication method that can be used to produce components having complex shapes from materials that are hard to machine, such as metal matrix composites and intermetallics. Use of superplastic forming may become even more widespread if lower deformation temperatures can be attained. Here we present observations of low-temperature superplasticity in nanocrystalline nickel, a nanocrystalline aluminium alloy (1420-Al), and nanocrystalline nickel aluminide (Ni_3Al). The nanocrystalline nickel was found to be superplastic at a temperature 470 °C below that previously attained[2]: this corresponds to 0.36T_m, the lowest normalized superplastic temperature reported for any crystalline material. The nanocrystalline Ni_3Al was found to be superplastic at a temperature 450 °C below the superplastic temperature in the microcrystalline regime[3].

Since the introduction of nanocrystalline materials[4,5] and the progress in preparation techniques[6–8] for metals and alloys, many investigators have hoped to obtain superplasticity in pure metals and alloys with nanocrystalline structure at low temperature. This hope is broadly based on the fact that grain-boundary sliding is an important deformation mechanism during superplasticity. Related to grain-boundary sliding is a grain-size effect that is manifested as a decrease in superplastic temperature or flow stress, or as an increase in the superplastic strain rate, with reduction in grain size[1]. For this reason, interest in nanocrystalline materials has been shared by scientists working on superplasticity, because the large volume fraction of grain boundaries in nanostructured materials could lead to low-temperature or high-strain-rate superplasticity, in addition to providing new possibilities of studying grain-boundary-related phenomenon. The work presented here represents a large part of the total experimental data collected to date on superplastic behaviour in such systems.

Tensile samples having a gauge length and width of 1.0 mm, with a nominal thickness of 0.2 mm, were machined by electro-discharge from nickel, 1420-Al and Ni_3Al. The nickel was electrodeposited, and had a purity of greater than 99.5%. The 1420-Al and the Ni_3Al were processed by severe plastic deformation[6], and had compositions, in weight per cent, of Al-5Mg-2Li-0.1Zr and Ni-8.5Al-7.8Cr-0.6Zr-0.02B, respectively. Specimen size was dictated by

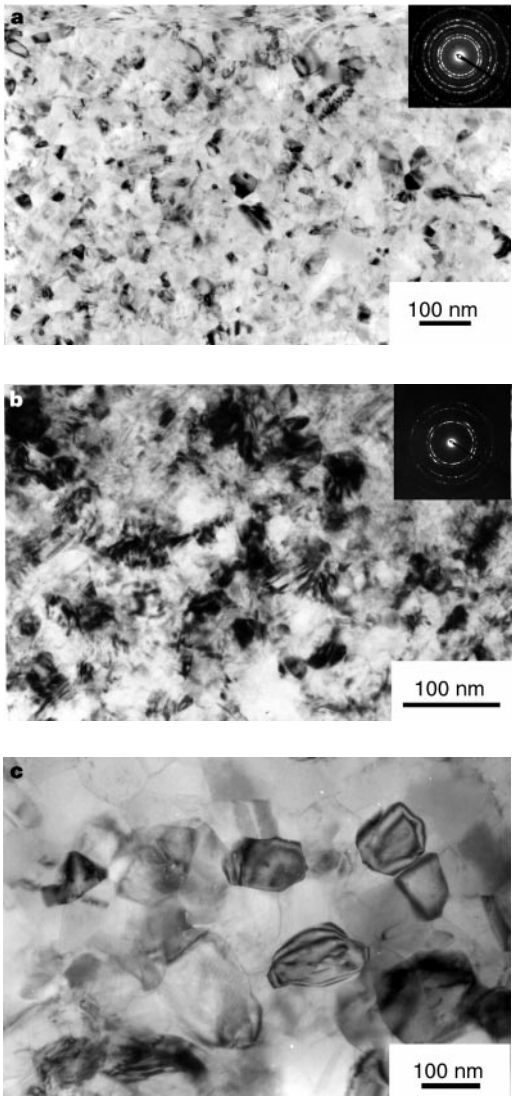

Figure 1 TEM images of the microstructures of the nanocrystalline metals and alloys investigated in this work. Bright-field micrographs show the microstructures of electrodeposited nickel (**a**), nickel aluminide, Ni_3Al, processed by severe plastic deformation (**b**), and Ni_3Al after superplastic deformation at 650 °C (**c**). Insets show the ring diffraction patterns, typical of nanostructured materials. Grain growth during deformation was limited in Ni_3Al.

limitations on the size of sample that could be processed by severe plastic deformation; in this process, small disks of 10–15 mm diameter are strained by torsion under high pressure.

As-processed grain sizes for the nickel, 1420-Al and Ni_3Al were 20 nm, 100 nm and 50 nm, respectively. Bright-field transmission electron micrographs of nickel and Ni_3Al are shown in Fig. 1. The tensile samples were deformed in tension at constant strain rates and temperatures. Data on the thermal stability of the nickel are available[9,10], and were confirmed in this work using electron microscopy of annealed samples, which showed that rapid grain growth began at 350 °C. Data on the thermal stability of the 1420-Al and Ni_3Al were collected using transmission electron microscopy (TEM) while heating *in situ*.

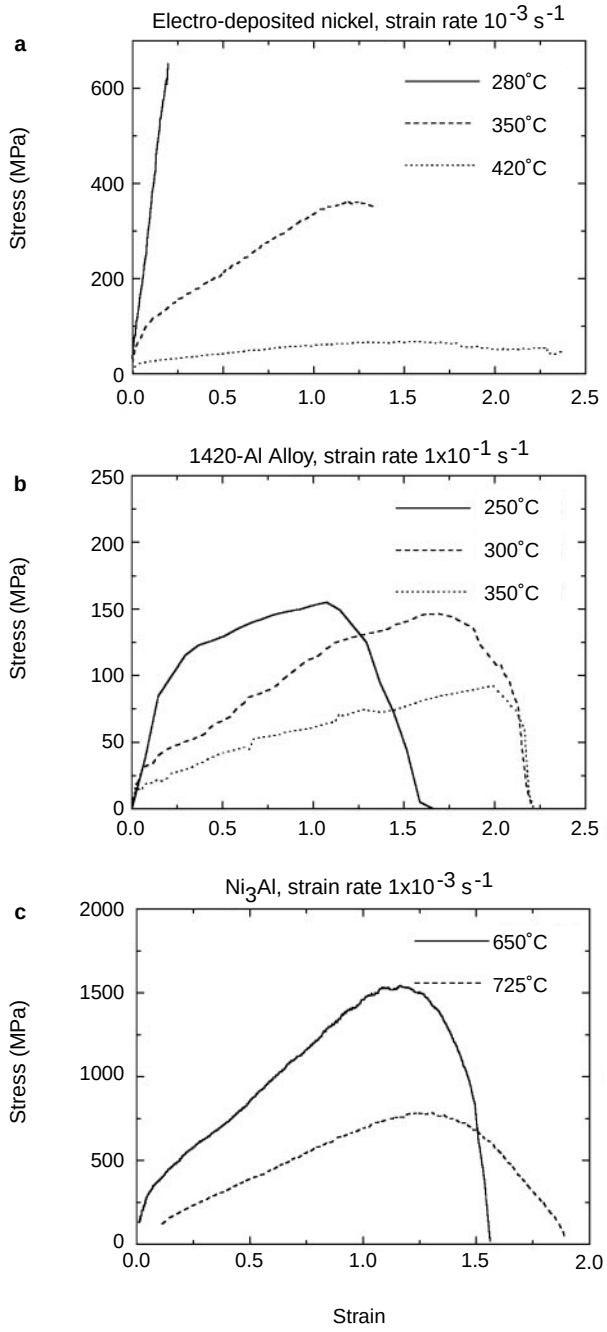

Figure 2 Stress–strain data obtained at constant strain rates and temperatures. Shown are stress–strain curves for electrodeposited nickel (**a**), aluminium alloy 1420-Al processed by severe plastic deformation (**b**), and Ni_3Al processed by severe plastic deformation (**c**). Note the transition from low plasticity to superplasticity in **a** between 280 °C and 350 °C, the high strain rates in **b**, and the very high flow stresses in **c**.

Stress–strain curves (Fig. 2) reveal some important features of the mechanical behaviour of these materials. In the case of nickel, a transition occurred above 280 °C; this is indicated by the curve for 350 °C, which shows yielding and strong strain hardening with a large increase in plastic deformation into the superplastic regime of >200% elongation[1]. Annealed microcrystalline nickel also exhibits a drop in yield strength and tensile strength within this temperature range[11], but the drop was much larger for the nanocrystalline samples and, more importantly, was accompanied by superplastic deformation not observed in larger-grained materials. This transition from low plasticity to superplasticity coincided with the onset of grain growth, and may be explained by a combination of the activation of grain-boundary sliding, increased diffusion, and increased ease of dislocation generation.

The stress–strain curves for nickel, 1420-Al and Ni_3Al demonstrated significant work hardening, and flow stresses were higher than those observed[3] for superplastic deformation of microcrystalline states. Microcrystalline Ni_3Al has a yield-stress maximum[12] around 650 °C, referred to in the literature as a "yield stress anomaly", but this strength maximum is accompanied by a ductility minimum, around 20% total elongation. However, in nanocrystalline Ni_3Al we achieved a tensile ductility of 350% at this temperature. As indicated in Fig. 2, in addition to lower superplastic temperatures 1420-Al also demonstrated high-strain-rate superplasticity, defined by superplastic strain rates greater than 10^{-2} s^{-1}. Such behaviour in a microcrystalline 1420-Al alloy has been reported by Berbon *et al.*[13]. The combination of low-temperature and high-strain-rate superplasticity is significant, and may have technological implications for superplastic forming. Samples before and after deformation are shown in Fig. 3, which demonstrates the large uniform elongation representative of superplasticity.

Based on the heating profile for the tests of nickel at 350 °C, samples were annealed to determine grain size at the start of deformation. The resulting microstructure consisted of a nanocrystalline matrix with isolated 0.3-μm grains. After deformation at 350 °C, the average grain size in the deformed gauge section was 1.3 μm along the tensile axis and 0.64 μm transverse to the tensile axis. Although significant grain growth occurred during deformation, these grain sizes were still much smaller than those which are obtainable using conventional refinement techniques[14]. Heating experiments showed that the grain size of 1420-Al and Ni_3Al was unchanged by heating to the respective test temperatures of 250 °C and 650 °C, but that internal strains were reduced, as shown by sharper grain contrast in TEM images. After testing 1420-Al at 250 °C, the grain size in the deformed gauge section was 0.22 μm. Thus, some grain growth occurred during deformation but not to the extent as in electro-deposited nickel. After Ni_3Al was tested at 650 °C, the grain size in the deformed gauge section was 100 nm

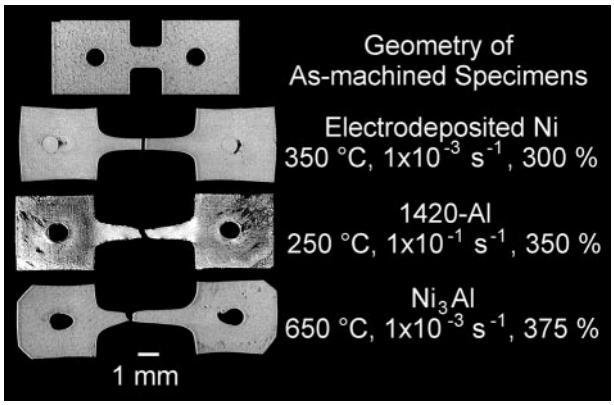

Figure 3 Miniature tensile specimens, shown in the as-machined geometry, and after deformation.

(Fig. 1c). Therefore, Ni_3Al remained nanocrystalline throughout the deformation. This observation has significance regarding the deformation mechanism. The common explanation of strain hardening during superplasticity at constant strain rate and temperature is that grain growth increases the flow stress through grain-size sensitivity, where stress is proportional to grain size. But at 650 °C, the flow stress for nanocrystalline Ni_3Al increased six-fold between the yield stress and the peak stress, while the grain size increased only two-fold. This suggests that mechanistic details of superplasticity in nanocrystalline materials are fundamentally different from those in microcrystalline materials. A detailed microstructural investigation is required to explain the high strain hardening observed during superplasticity.

From the stress–strain curves, it is clear that the maximum elongation for each material was found at higher temperatures than those discussed above. The reason for focusing on the lower temperatures is to investigate the effect of nanostructure, and to probe the low-temperature limits of superplasticity. At higher temperatures, grain growth shifts the microstructure into the submicrocrystalline range. Furthermore, the practical advantages of superplastic deformation are not necessarily lost by operating away from the ductility maximum, as deformation in the range of a few hundred per cent is all that is required for many commercial forming operations.

Our experimental results allow us to make some observations about superplasticity in nanocrystalline metals and alloys. The single most significant observation is the large reduction in superplastic temperatures. In the case of nickel, an extremely low normalized temperature was attained. But even at very low temperatures, grain growth during deformation of nanostructured nickel resulted in a grain size larger than the commonly used definition for nanostructured materials of 100 nm or less. The primary reason for such growth is a large driving force resulting from grain-boundary energy. These results appear to eliminate the hope of obtaining superplasticity in pure metals having a grain size of 100 nm or less, because the reduction of superplastic temperature is offset by a reduction in the grain-growth temperature. However, secondary factors such as internal strain energy may influence the grain-growth temperature through contributions to the driving force, and these effects have not yet been evaluated.

Even if secondary contributions to grain growth could be eliminated, grain-growth and superplastic temperatures cannot be treated independently because both are thermally activated processes linked closely through solid-state diffusion. Therefore, in the limiting case of nanostructured pure metals, grain growth will occur if sufficient thermal activation is present for superplastic deformation. This competition between grain growth and superplasticity was established early in the development of the field, but has not hitherto been investigated at such small starting grain size.

Grain growth is commonly controlled with multiple-phase alloys, where second phases are present as particles or individual grains. Particles inhibit grain growth by pinning the boundaries, while two-phase systems require diffusion through neighbouring grains of different composition to accommodate growth. These effects can be seen by comparing the grain growth during deformation between nanocrystalline nickel and 1420-Al (data not shown), where the increase in grain size of nickel was more than that of 1420-Al even though nickel was at a lower normalized temperature. In the case of ordered intermetallics, such as Ni_3Al, grain growth is inhibited by the kinetic barrier of preferred atomic pairing between the species present, and the grain-size stability of the Ni_3Al is attributed to this effect.

Investigation of superplasticity in nanostructured materials is still in its infancy, and many systems exist that hold promise for superplastic behaviour while retaining a grain size of 100 nm or less. The small number of experimental results on superplasticity obtained from nanostructured materials have upheld predictions of low-temperature deformation, while at the same time the difficulty of maintaining a nanocrystalline grain size in pure nickel has emphasized the interaction of thermally activated processes in these materials. However, the high flow stresses and significant work hardening observed in Ni_3Al and 1420-Al have suggested that details of superplasticity are fundamentally different in nanostructured materials. □

Received 3 November 1998; accepted 19 February 1999.

1. Mukherjee, A. K. in *Materials Science and Technology* Vol. 6, *Plastic Deformation and Fracture of Materials* (ed. Mughrabi, H.) Ch. 9 (VCH, New York, 1993).
2. Floreen, S. Superplasticity in pure nickel. *Scripta Metall.* **1,** 19–23 (1967).
3. Mukhopadhyay, J., Kashner, G. & Mukherjee, A. K. Superplasticity in boron doped Ni_3Al alloy. *Scripta Metall. Mater.* **24,** 857–862 (1990).
4. Gleiter, H. Nanocrystalline materials. *Prog. Mater. Sci.* **33,** 223–315 (1989).
5. Suryanarayana, C. Nanocrystalline materials. *Int. Mater. Rev.* **40,** 41–64 (1995).
6. Valiev, R. Z. Ultrafine-grained materials produced by severe plastic deformation. *Ann. Chim.* **21,** 6–7, 369–378 (1996).
7. Birringer, R. & Gleiter, H. in *Encyclopedia of Material Science and Engineering: Supplement 1* (eds Cahn, R. W. & Beaver, M. B.) 339–349 (Pergamon, Oxford, 1988).
8. El-Sherik, A. M. & Erb, U. Synthesis of bulk nanocrystalline nickel by pulsed electrodeposition. *J. Mater. Sci.* **30,** 5743–5749 (1995).
9. Wang, N., Wang, Z., Aust, K. T. & Erb, U. Isokinetic analysis of nanocrystalline nickel electrodeposits upon annealing. *Acta Mater.* **45,** 1655–1669 (1997).
10. Natter, H., Schmeltzer, M. & Hempelmann, R. Nanocrystalline nickel and nickel copper alloys: Synthesis, characterisation, and thermal stability. *J. Mater. Res.* **13,** 1186–1197 (1998).
11. Everhart, J. L. *Engineering Properties of Nickel and Nickel Alloys* 20 (Plenum, New York, 1971).
12. Liu, V. T. & Sikka, V. Nickel aluminides for structural use. *J. Metals* **38,** 19–21 (1987).
13. Berbon, P. B. *et al.* Fabrication of bulk ultrafine-grained materials through intense plastic straining. *Metall. Mater. Trans. A* **29,** 2237–2243 (1998).
14. Kaybyshev, O. A. & Mareklov, A. A. Structural changes during superplastic deformation of nickel and chromium. *Fiz. Metal. Metalloved.* **41,** 190–196 (1976).

Acknowledgements. This work was supported by the US National Science Foundation and the Civil Research and Development Foundation.

Correspondence and requests for materials should be addressed to A.K.M. (e-mail: akmukherjee@ucdavis.edu).

Stochastic sensing of organic analytes by a pore-forming protein containing a molecular adapter

Li-Qun Gu*, Orit Braha*, Sean Conlan*, Stephen Cheley* & Hagan Bayley*†

** Department of Medical Biochemistry & Genetics, Texas A&M University Health Science Center, 440 Reynolds Medical Building, College Station, Texas 77843-1114, USA*

† Department of Chemistry, Texas A&M University, College Station, Texas 77843-3255, USA

The detection of organic molecules is important in many areas, including medicine, environmental monitoring and defence[1–5]. Stochastic sensing is an approach that relies on the observation of individual binding events between analyte molecules and a single receptor[6]. Engineered transmembrane protein pores are promising sensor elements for stochastic detection[6], and in their simplest manifestation they produce a fluctuating binary ('on/off') response in the transmembrane electrical current. The frequency of occurrence of the fluctuations reveals the concentration of the analyte, and its identity can be deduced from the characteristic magnitude and/or duration of the fluctuations. Genetically engineered versions of the bacterial pore-forming protein α-haemolysin have been used to identify and quantify divalent metal ions in solution[6]. But it is not immediately obvious how versatile binding sites for organic ligands might be obtained by engineering of the pore structure. Here we show that stochastic sensing of organic molecules can be procured from α-haemolysin by equipping the channel with an internal, non-covalently bound molecular 'adapter' which mediates channel blocking by the analyte. We use cyclodextrins as the adapters because these fit